Article

Monolayer-Protected Nanoparticle Film Assemblies as Platforms for Controlling Interfacial and Adsorption Properties in Protein Monolayer Electrochemistry

Andrew F. Loftus, Katelyn P. Reighard, Susanna A. Kapourales, and Michael C. Leopold

J. Am. Chem. Soc., **2008**, 130 (5), 1649-1661 • DOI: 10.1021/ja076312k

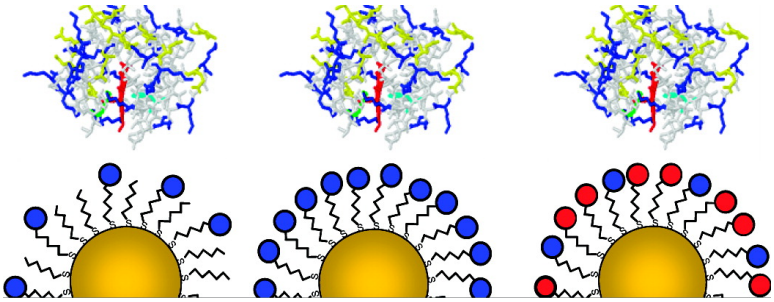

J|A|C|S
ARTICLES
Published on Web 01/12/2008

Monolayer-Protected Nanoparticle Film Assemblies as Platforms for Controlling Interfacial and Adsorption Properties in Protein Monolayer Electrochemistry

Andrew F. Loftus, Katelyn P. Reighard, Susanna A. Kapourales, and Michael C. Leopold*

Department of Chemistry, Gottwald Center for the Sciences, University of Richmond, Richmond, Virginia 23173

Received August 22, 2007; E-mail: mleopold@richmond.edu

Abstract: Assembled films of nonaqueous nanoparticles, known as monolayer-protected clusters (MPCs), are investigated as adsorption platforms in protein monolayer electrochemistry (PME), a strategy for studying the electron transfer (ET) of redox proteins. Modified electrodes featuring MPC films assembled with various linking methods, including both electrostatic and covalent mechanisms, are employed to immobilize cytochrome *c* (cyt *c*) for electrochemical analysis. The background signal (non-Faradaic current) of these systems is directly related to the structure and composition of the MPC films, including nanoparticle core size, protecting ligand properties, as well as the linking mechanism utilized during assembly. Dithiol-linked films of $Au_{225}(C6)_{75}$ are identified as optimal films for PME by sufficiently discriminating against detrimental background current and exhibiting interfacial properties that are readily engineered for cyt *c* adsorption and electroactivity (Faradaic current). Surface concentrations and denaturation rates of adsorbed cyt *c* are dictated by specific manipulation of the individual MPCs composing the outer layer of the film. The use of specially designed, hydrophilic MPCs as a terminal film layer results in near-ideal cyt *c* voltammetry, attributed to a high degree of molecular level control of the necessary interfacial interactions and flexibility needed to create a uniform and effective binding of protein across large areas of a substrate. The electrochemical properties of cyt *c* at MPC films, including ET rate constants that are unaffected by the large ET distance introduced by MPC assemblies, are compared to traditional strategies employing self-assembled monolayers to immobilize cyt *c*. The incorporation of nanoparticles as protein adsorption platforms has implications for biosensor engineering as well as fundamental biological ET studies.

Introduction

The successful immobilization of biomolecules onto synthetic substrates is a critical, fundamental event for many aspects of bioanalytical chemistry, including biosensor engineering,[1−5] biological electron transfer (ET) modeling systems,[6] bioseparations,[7] and the development of biocompatible materials.[8] It follows that molecular level control and understanding of the interactions between biomolecules and synthetic materials is an important factor in developing these technologies toward specific goals such as the miniaturization and implantation of in vivo, amperiometric biosensors.[3] Moreover, the ability to easily implement a uniform surface environment for the adsorption of biomolecules across a large surface area is of both fundamental and practical interest. Significant research efforts have focused on understanding and controlling protein adsorption at man-made substrates either as a precursor to a biosensor design or as a means of exploring fundamental properties of biological systems.[9] A prominent example of this type of research is the direct or unmediated electrochemistry of redox-active proteins at modified electrodes.[10,11]

The direct electrochemistry of electroactive proteins can be used to study the ET processes of many vital physiological events such as mitochondrial respiration and photosynthesis.[6] Strategies to study these phenomena have steadily evolved over the years to the current practice of performing heterogeneous electrochemistry with solid electrodes serving as redox partners for the proteins, a popular technique called protein monolayer electrochemistry (PME).[12−20] This heterogeneous and diffusionless strategy simplifies the redox reaction by confining a

(1) Scouten, W. H.; Luong, J. H.; Brown, R. S. *Trends Biotechnol.* **1995**, *13*, 178−185.
(2) Davis, J.; Vaughan, D. H.; Cardosi, M. F. *Enzyme Microb. Technol.* **1995**, *17*, 1030−1035.
(3) *Commercial Biosensors: Applications to Clinical, Bioprocess, and Environmental Samples;* Ramsay, G., Ed.; Wiley: New York, 1998.
(4) Ghindilis, A. L.; Atanasov, P.; Wilkins, E. *Biosens. Bioelectron.* **1998**, *13*, 113−131.
(5) Nam, J.; Shad, T. C.; Mirkin, C. A. *Science* **2003**, *301*, 1884.
(6) Bowden, E. F. *Electrochem. Soc. Interface* **1997**, *6*, 40−44.
(7) Oscarsson, S. *J. Chromatogr., B* **1997**, *699*, 117−131.
(8) Schoenfisch, M. H.; Mowery, K. A.; Rader, M. V.; Baliga, N.; Wahr, J. A.; Meyerhoff, M. E. *Anal. Chem.* **2000**, *72*, 1119−1126.
(9) Mrksich, M.; Whitesides, G. M. *Annu. Rev. Biophys. Biomol. Struct.* **1996**, *25*, 55−78.
(10) Heller, A. *J. Phys. Chem.* **1992**, *96*, 3579−3587.
(11) Armstrong, F. A.; Hill, H.; Allen O.; Walton, N. J. *Acc. Chem. Res.* **1988**, *21*, 407−413.
(12) Kuwana, T.; Yeh, P. *Chem. Lett.* **1977**, 1145−1148.
(13) Landrum, H. L.; Salmon, R. T.; Hawkridge, F. M. *J. Am. Chem. Soc.* **1977**, *99*, 3154−3158.
(14) Bowden, E. F.; Clark, R. A.; Willit, J. L.; Song, S. *Proc.—Electrochem. Soc.* **1993**, *93−11*, 34−45.

monolayer of protein to the electrode surface, eliminating the kinetics of adsorption/desorption and effectively isolating the ET step. Aside from the simplified kinetics, PME offers the advantage of potentiostatic control over the free energy of the ET reaction that facilitates the measurement of valuable thermodynamic and kinetic parameters including, for example, formal potential, reorganization energy, and ET rate constants.[14]

The immobilization of redox-active proteins onto a substrate is considered a mimic of important protein/protein complexes in living organisms,[21,22] a concept applicable to biosensor designs that rely on such interactions. Thus, PME systems can serve as models for investigating protein adsorption processes and monitoring changes in the immobilized protein's structure and function through relatively simple electrochemical analysis. It follows that the electrode interface must be designed to promote protein adsorption without immediate denaturation, a common phenomenon of proteins at metal electrodes.[9,21,23−26] Specially modified electrodes have been designed to mimic protein binding interfaces and promote the adsorption of stable monolayers of native protein. One important example of modifiers used for this purpose is alkanethiolate-based self-assembled monolayers (SAMs) which provide a highly ordered interfacial environment that sustains adsorbed protein electroactivity.[27] Additionally, the synthetic options of altering chain length and terminal groups of the ω-substituted alkanethiol components allow for study of ET distance dependence and interfacial engineering to maximize the adsorbed protein's electronic coupling to the electrode.[28]

As PME strategies were employed, several key disadvantages of the approach also emerged.[14] Because of the inherent design of PME systems, adsorption is limited to a monolayer or less of coverage. Consequently, the analytical signal from the protein layer, the Faradaic current, is restricted to a relatively low signal-to-background ratio. Modified electrode systems with larger background signals, also known as charging current or capacitance, can obscure the protein electrochemistry, making quantitative measurements problematic and less accurate. To combat this limitation, alkanethiolate SAMs are again useful, offering effective background discrimination with their tightly packed, low dielectric hydrocarbon layers. Likewise, the application of pulsed electrochemical techniques improves signal definition in systems where high background currents persist. In spite of these advancements, any type of innovation regarding the modified electrode interface in PME must still consider the critical issue of background compensation.[14]

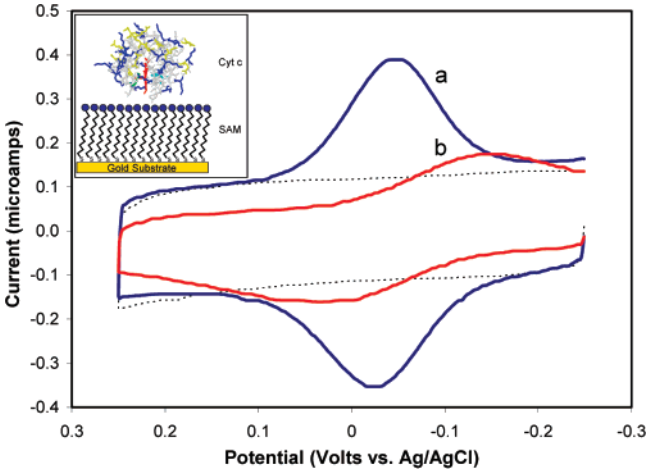

Figure 1. Cyclic voltammetry of cyt *c* adsorbed at SAMs of (a) MUA and (b) MHDA in 4.4 mM potassium phosphate buffer (pH = 7) at 100 mV/s. The non-Faradaic background, or charging current, is shown (dashed line) for the MUA SAM and is directly proportional to the C_{dl} of the films. Inset: Schematic of traditional PME strategy where cyt *c*, having an asymmetric charge distribution (positively charged (lysines and arginines) and negatively charged (aspartates and glutamates) shown in blue and yellow, respectively), is adsorbed to a carboxylic acid-terminated SAM.

Another limitation of PME systems is the nature of the electrochemical results obtained with this strategy. Ideally, PME systems would feature surface-confined protein that is uniformly adsorbed with identical orientations. The reality of PME systems, however, is far from these conditions. To illustrate this concept, one need only examine a well-developed PME system, cytochrome *c* (cyt *c*) adsorbed to carboxylic acid-terminated SAMs, illustrated in Figure 1, inset. Cyt *c* is well-characterized featuring an asymmetric amino acid charge distribution about the heme group that lends itself to adsorption at anionic surfaces.[29] Although the voltammetry of this system reveals a strong electrochemical response from the adsorbed protein (Figure 1), it also deviates significantly from electrochemical theory of adsorbed species. Specifically, the voltammetry displays anomalous peak broadening with significantly larger full width at half-maximum (fwhm) values than predicted for ideally adsorbed systems (90 mV).[30] A key report by Clark and Bowden examined the sources of the nonideality and identified a heterogeneous population of cyt *c* adsorbates at the SAM interface as a major factor causing the dispersion of electrochemical properties.[31] A later report by the same group showed that gold substrate topography significantly affects the defect density of the SAM and contributes to the interfacial heterogeneity.[32] Studies of cyt *c* voltammetry at SAMs of varying chain lengths found the voltammetric broadening was more significant in systems with more structural order (longer chain lengths) as they are more sensitive to surface topography (Figure 1).[31] Bowden and co-workers also showed that the use of mixed SAMs, varying in both chain length and endgroup, resulted in superior electronic coupling of cyt *c* compared to that of uniform SAMs.[28,31]

On the basis of the literature described here, it appears that more ideal cyt *c* voltammetry can be achieved by engineering

(15) Cherry, R. J.; Bjornsen, A. J.; Zapien, D. C. *Langmuir* **1998**, *14*, 1971−1973.
(16) Xu, J.; Bowden, E. F. *J. Am. Chem. Soc.* **2006**, *128*, 6813−6822.
(17) Zhang, J.; Christensen, H. E. M.; Ooi, B. L.; Ulstrup, J. *Langmuir* **2004**, *20*, 10200−10207.
(18) Liu, G. Z.; Gooding, J. J. *Langmuir* **2006**, *22*, 7421−7430.
(19) Baker, S. E.; Colavita, P. E.; Tse, K.; Hamers, R. J. *Chem. Mater.* **2006**, *18*, 4415−4422.
(20) Nakano, K.; Yoshitake, T.; Yamashita, Y.; Bowden, E. F. *Langmuir* **2007**, *23*, 6270−6275.
(21) Willit, J. L.; Bowden, E. F. *J. Phys. Chem.* **1990**, *94*, 8241−8246.
(22) Garber, E. A. E.; Margoliash, E. *Biochim. Biophys. Acta* **1990**, *1015*, 279−287.
(23) Wahlgren, M.; Arnebrant, T. *Trends Biotechnol.* **1991**, *9*, 201−208.
(24) Sagara, T.; Niwa, K.; Sone, A.; Hinnen, C.; Niki, K. *Langmuir* **1990**, *6*, 254−262.
(25) Prime, K. L.; Whitesides, G. M. *Science* **1991**, *252*, 1164−1167.
(26) Ostuni, E.; Grzybowski, B. A.; Mrksich, M.; Roberts, C. S.; Whitesides, G. M. *Langmuir* **2003**, *19*, 1861−1872.
(27) Song, S.; Clark, R. A.; Bowden, E. F.; Tarlov, M. J. *J. Phys. Chem.* **1993**, *97*, 6564−6572.
(28) Kasmi, A. E.; Wallace, J. M.; Bowden, E. F.; Binet, S. M.; Linderman, R. J. *J. Am. Chem. Soc.* **1998**, *120*, 225−226.
(29) Pettigrew, G. W.; Moore, G. R. *Cytochromes c: Biological Aspects;* Springer-Verlag: Berlin, 1990.
(30) Bard, A. J.; Faulkner, L. R. *Electrochemical Methods: Fundamentals and Applications;* Wiley: New York, 1980.
(31) Clark, R. A.; Bowden, E. F. *Langmuir* **1997**, *13*, 559−565.
(32) Leopold, M. C.; Bowden, E. F. *Langmuir* **2002**, *18*, 2239−2245.

an interface that possesses a chemically diverse but uniform adsorption environment for the protein while simultaneously negating substrate topography.[31,32] Achieving this goal requires a system that offers greater molecular level control of the protein−substrate junction over a large area of the electrode, including homogeneous adsorption sites that offer a specific combination of intermolecular interactions (Coulombic and hydrophobic) and flexibility to promote native protein adsorption. The construction of an adsorption platform with these properties that does not sacrifice the convenience and effectiveness of the PME strategy and yet is still able to facilitate ET reactions of the adsorbed protein is a formidable challenge.

Colloidal gold nanoparticles (NPs) have been the subject of significant research attention in recent years as a potential scaffold for supporting protein adsorption.[33,34] For the purpose of immobilizing protein in potential biosensor designs, many researchers have noted that NPs offer several unique advantages, including large surface-to-volume ratios that yield high areas of contact for adsorbates, readily manipulated properties such as core size and peripheral functionalization, an increase in freedom of orientation for adsorbed biomolecules, and an ability to act as conductive pathways for ET reactions.[35,36] Early work by Crumbliss et al.[37] established that proteins and enzymes adsorbed to nanoparticles maintain their electrochemical activity. Since that time, several strategies of incorporating commonly used citrate-stabilized nanoparticles (CS-NPs) into electrochemical biosensors have been employed, including the direct attachment of CS-NPs to electrodes or the incorporation of CS-NPs into an electrode's matrix coating where biomolecules are directly adsorbed or cross-linked.[38−42] Slow ET kinetics and complications from an enhanced charging current, common to CS-NPs, were observed in these studies.

The alternative strategy for the direct electrochemistry of adsorbed proteins is to immobilize protein at an electrode modified with a CS-NP film. Although limited in number, studies of this nature include examining adsorbed myoglobin, hemoglobin, and horseradish peroxidase at CS-NP-modified electrodes of various materials.[43−45] While direct electrochemistry was achieved in these reports, the voltammetry was not nearly ideal, exhibiting diffusion-limited instead of classically adsorbed current responses, elevated background signals, and quasi-reversible kinetics. The direct electrochemistry of cyt *c* at NP films has also been investigated by several groups. A report by Natan and co-workers[46] achieved diffusional voltammetry of cyt *c* at SnO_2 electrodes modified with CS-NPs and noted an interesting dependence of ET kinetics on the diameter of the NPs, suggesting nanometer-scale morphology has a substantial effect on the protein electrochemistry. Researchers have explored adsorbed systems as well, with Scheller's lab modifying electrodes with a mixture of CS-NPs in carbon paste as an adsorption platform for cyt *c*.[47] Chen and co-workers[48,49] followed with cyt *c* adsorbed to films of chitosan-stabilized NPs at cysteine-modified gold. Most recently, Dong et al. examined cyt *c* immobilized on a film of CS-NPs supported by an aromatic SAM-modified glassy carbon electrode.[50,51] While successful at attaining cyt *c* electrochemistry, most of these reports featured voltammetry that was less than ideal in some aspect, including poorly defined peaks, erratic backgrounds, poor stability, and quasi-reversible ET kinetics.[52−54] In spite of these efforts, PME of cyt *c* at NP films remains a system that can be further optimized.

In this study, we investigated assembled films of alkanethiol-protected NPs, known as monolayer-protected clusters (MPCs),[55,56] as a component of cyt *c* PME. A primary objective was to determine if specific engineering of individual MPC properties composing the film would translate into molecular level control at the interface and affect cyt *c* adsorption and electrochemistry. Of interest to the research community for some time, MPCs (pictured in Scheme 1) are specifically targeted here because of their unique structural properties that are readily manipulated via synthesis and chemical treatment, including the core size and composition of peripherial ligands. These engineering options should allow for a high level of control over the interfacial flexibility, functionality, and uniformity of the protein adsorption platform. To the best of our knowledge, this is the first report to explore the potential of alkanethiol MPCs in this capacity and to this depth.[36,57,58] This research seeks to provide a straightforward and effective strategy for controlling and understanding protein adsorption at a surface, a goal that may ultimately benefit many aspects of bioanalytical technology.

Experimental Details

Chemicals. Unless otherwise noted, all chemicals were of reagent grade and used as received. All solutions were made with 18 MΩ ultrapurified water (PureLab-Ultra, Elga).

MPC Synthesis and Functionalization. Alkanethiolate-based MPCs were synthesized using variations of the well-established Brust reac-

(33) Niemeyer, M. *Angew. Chem., Int. Ed.* **2001**, *40*, 4128−4158.
(34) Shenhar, R.; Rotello, V. M. *Acc. Chem. Res.* **2003**, *36*, 549−561.
(35) Yanez-Sedeno, P.; Pingarron, J. M. *Anal. Bioanal. Chem.* **2005**, *382*, 884−886.
(36) You, C.; De, M.; Han, G.; Rotello, V. M. *J. Am. Chem. Soc.* **2005**, *127*, 12873−12881.
(37) Zhao, J.; Henkens, R. W.; Stonehuerner, J.; O'Daly, J. P.; Crumbliss, A. L. *J. Electroanal. Chem.* **1992**, *327*, 109−119.
(38) Zhang, H.; Lu, H.; Hu, N. *J. Phys. Chem. B* **2006**, *110*, 2171−2179.
(39) Jia, J.; Wang, B.; Wu, A.; Cheng, G.; Li, Z.; Dong, S. *Anal. Chem.* **2002**, *74*, 2217−2223.
(40) Yang, W.; Wang, J.; Zhao, S.; Sun, Y.; Sun, C. *Electrochem. Commun.* **2006**, *8*, 665−672.
(41) Wang, L.; Wang, E. *Electrochem. Commun.* **2004**, *6*, 49−54.
(42) Jena, B. K.; Raj, C. R. *Anal. Chem.* **2006**, *78*, 6332−6339.
(43) Zhang, J.; Oyama, M. *J. Electroanal. Chem.* **2005**, *577*, 273−279.
(44) Han, X.; Cheng, W.; Zhang, Z.; Dong, S.; Wang, E. *Biochim. Biophys. Acta* **2002**, *1556*, 273−277.
(45) Yi, X.; Ju, H.; Chen, H. *Anal. Biochem.* **2000**, *278*, 22−28.
(46) Brown, K. R.; Fox, A. P.; Natan, M. J. *J. Am. Chem. Soc.* **1996**, *118*, 1154−1157.
(47) Ju, H.; Liu, S.; Ge, B.; Lisdat, F.; Scheller, F. W. *Electroanalysis* **2002**, *14*, 141−147.
(48) Gu, H.-Y.; Yu, A.-M.; Chen, H.-Y. *J. Electroanal. Chem.* **2001**, *516*, 119−126.
(49) Feng, J.-J.; Zhao, G.; Xu, J.-J.; Chen, H.-Y. *Anal. Biochem.* **2005**, *342*, 280−286.
(50) Jiang, X.; Shang, L.; Wang, Y.; Dong, S. *Biomacromolecules* **2005**, *6*, 3030−3036.
(51) Jiang, X.; Zhang, L.; Jiang, J.; Qu, X.; Wang, E.; Dong, S. *ChemPhysChem* **2005**, *6*, 1613−1621.
(52) Some of the systems were stable for only short periods of time, and the use of cyt *c* as received (i.e., not purified) is not recommended as it may significantly influence the observed voltammetry. Moreover, on the basis of a seminal report by Natan et al.[53] and work in our own laboratory,[54] there is also a legitimate concern that films of citrate-stabilized nanoparticles are inherently unstable and readily aggregate upon placement on a substrate or during assembly into multilayers.
(53) Musick, M. D.; Keating, C. D.; Lyon, L. A.; Botsko, S. L.; Pena, D. J.; Holliway, W. D.; McEvoy, T. M.; Richardson, J. N.; Natan, M. J. *Chem. Mater.* **2000**, *12*, 2869−2881.
(54) Russell, L. E.; Galyean, A. A.; Notte, S. M.; Leopold, M. C. *Langmuir* **2007**, *23*, 7466−7471.
(55) Templeton, A. C.; Wuelfing, W. P.; Murray, R. W. *Acc. Chem. Res.* **2000**, *33*, 27−36.
(56) Wuelfing, W. P.; Zamborini, F. P.; Templeton, A. C.; Wen, X.; Yoon, H.; Murray, R. W. *Chem. Mater.* **2001**, *13*, 87−95.
(57) Rotello and coworkers have done excellent work exploring protein interactions with MPCs of this nature in solution[36,58] but did not expand their work to a film geometry.
(58) Boal, A. K.; Rotello, V. M. *J. Am. Chem. Soc.* **1999**, *121*, 4914−4915.

Scheme 1. MPC Networked Film Assembly as a Protein Adsorption Platform

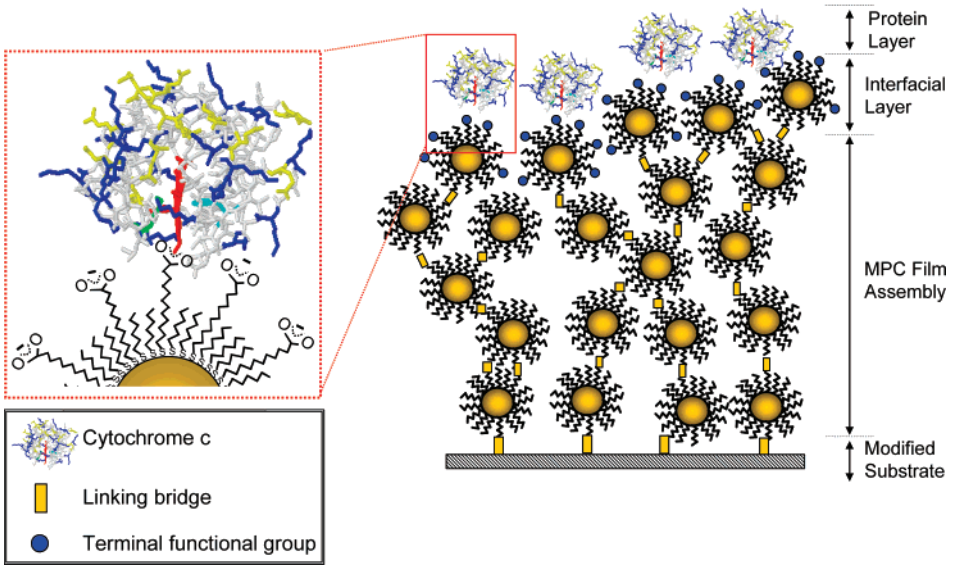

tion.[59] MPC core size was controlled by altering thiol-to-gold ratios, temperature, and reactant delivery rate during the reaction.[55] In a brief description of the MPC synthetic procedure, an aqueous solution of gold salt, $HAuCl_4$, was treated with tetraoctylammonium bromide in toluene to phase transfer the gold into the organic layer. Stoichiometric amounts of thiol were then added to the organic layer, which was stirred for at least 30 min while Au(I) polymer formed in solution as indicated by a distinct color change from orange/red to clear or pale yellow (depending on the amount of thiol added). After the solution was brought to the desired reaction temperature, aqueous $NaBH_4$ was added to reduce Au(I) to metallic gold in the presence of thiols and form a thick black solution of MPCs in toluene. The reaction was allowed to proceed overnight before the organic layer was rotary-evaporated to dryness, precipitated with acetonitrile, recollected on a glass frit, and washed with copious amounts of acetonitrile. Modifications to the Brust synthesis (e.g., thiol/Au ratios, temperature, rate of reactant introduction) allowed for the creation of MPCs with *average* core diameters between 0.9 and 5.2 nm, easily spanning the ~3.5-nm diameter of cyt *c*, the targeted protein. Thiol-to-gold ratios of 3:1, 2:1, and 1:1 were used to produce MPCs with average predominant cores of Au_{140}, Au_{225}, and Au_{807}, respectively.[60,61] The average diameter of the MPCs produced was verified with TEM imaging (Supporting Information).

MPCs were functionalized to varying degrees via place-exchange techniques that have been reported previously.[62] In brief, MPCs were co-dissolved with ω-substituted alkanethiols (e.g., 11-mercaptoundecanoic acid, MUA), which were subsequently exchanged from solution with surface-bound thiolates, resulting in a functionalized MPC. The extent of exchange was controlled by varying the reaction times and ratio of functionalized thiols to thiolates on the core. The approximate (average) compositions of the resulting functionalized MPCs were determined via NMR analysis of samples after iodine-induced oxidative decomposition, as previously described.[55,63]

Substrate Modification and MPC Film Assembly. Evaporated gold substrates (Evaporated Metal Films), mounted in previously designed electrochemical cells (described below), were electrochemically cleaned according to established procedures and immediately exposed to an ethanol solution of a specific thiol for 12 h (for shorter thiols) or up to 48 h (for longer thiols) to form SAMs on the surface.[64,65] For traditional PME systems (i.e., cyt *c* at SAM-modified electrodes, Figure 1), the SAMs were rinsed thoroughly with ethanol, water, and potassium phosphate buffer (KPB) before being exposed to a buffered protein solution for 1 to 2 h. Gold substrates to be used for MPC film assembly were electrochemically cleaned and modified with a SAM as an initial step for MPC film assembly. Beyond this initial modification of the gold surface, MPC films were assembled using "dipping cycles" that have been reported in detail elsewhere for each type of networked film (metal-linked,[66,67] ester-coupled,[68] and dithiol-linked[69]). Briefly, a single "dipping cycle" consists of exposure of the substrate to a solution of linking ligands followed immediately by exposure to a solution of MPCs. Within the electrochemical cells (described below) housing the gold substrates, dip cycles were performed by first filling the cell with one of the two solutions (e.g., linker) and stirring for a period of time by bubbling nitrogen into the cell. The cell was then thoroughly rinsed with CH_2Cl_2, and the process was repeated with the other solution (MPC). Brief summaries of each film's assembly procedure as well as atomic force microscopy (AFM) analysis of the films are included as part of the Supporting Information. For dithiol-linked films, this process was repeated for four dipping cycles with unfunctionalized MPCs before a final, fifth dipping cycle was used to deposit a functionalized layer designed for cyt *c* adsorption. The final layer is specifically designed to immobilize the ET protein cyt *c*, normally incorporating MUA ligands ($pK_a \approx 4-5$),[70] into the MPCs composing the final layer of the film (Scheme 1). Adsorption of the cationic cyt *c* at the MPC acid binding sites is followed by an electrochemical analysis of the adsorbed

(59) Brust, M.; Walker, M.; Bethell, D.; Schriffrin, D. J.; Whyman, R. J. *J. Chem. Soc., Chem. Commun.* **1994**, 801.
(60) Hostetler, M. J.; Wingate, J. E.; Zhong, C.-J.; Harris, J. E.; Vachet, R. W.; Clark, M. R.; Londono, J. D.; Green, S. J.; Stokes, J. J.; Wignall, G. D.; Glish, G. L.; Porter, M. D.; Evans, N. D.; Murray, R. W. *Langmuir* **1998**, *14*, 17−30.
(61) Wolfe, R. L.; Murray, R. W. *Anal. Chem.* **2006**, *78*, 1167−1173.
(62) Ingram, R. S.; Hostetler, M. J.; Murray, R. W. *J. Am. Chem. Soc.* **1997**, *119*, 9175−9178.
(63) These compositions are reported as *averages* because the polydispersity inherent in MPC samples introduces some degree of variability in core size and, as a consequence, the exact extent of exchange.
(64) SAMs composed of shorter chain-length thiolates tend to be inherently disordered regardless of deposition time, whereas films created from longer chain thiols require longer periods of time to become structurally ordered and stable.[65]
(65) Finklea, H. O. *Electroanal. Chem.* **1996**, *19*, 109−335.
(66) Zamborini, F. P.; Hicks, J. F.; Murray, R. W. *J. Am. Chem. Soc.* **2000**, *122*, 4514−4515.
(67) Sheibley, D.; Tognarelli, D. J.; Szymanik, R.; Leopold, M. C. *J. Mater. Chem.* **2005**, *15*, 491−498.
(68) Tognarelli, D. J.; Miller, R. B.; Pompano, R. R.; Loftus, A. F.; Sheibley, D. J.; Leopold, M. C. *Langmuir* **2005**, *21*, 11119−11127.
(69) Pompano, R. R.; Wortley, P. G.; Moatz, L. M.; Tognarelli, D. J.; Kittredge, K. W.; Leopold, M. C. *Thin Solid Films* **2006**, *510*, 311.
(70) Leopold, M. C.; Black, J. A.; Bowden, E. F. *Langmuir* **2002**, *18*, 978−980.

cyt *c* redox behavior and compared to the same experiment at a traditional PME system, cyt *c* adsorbed to a MUA SAM (Figure 1, inset).

Glass substrates were cleaned in "Piranha" solution (3:1, concentrated sulfuric acid/peroxide) before being silanized with 3-mercaptopropyltrimethoxysilane (3-MPTMS) to provide an exposed thiol for the immobilization of an initial layer of MPCs. WARNING: *Use extreme caution handling Piranha solution as it readily reacts with organic materials.* After the initial layer, a networked MPC film was assembled on silanized glass in a similar manner (i.e., dipping cycles) to the gold-supported MPC films described above.

Film Growth Monitoring and Characterization. MPC film growth on glass and gold substrates was monitored as described in the text with an Agilent UV−vis photodiode array spectrometer by recording the film's absorbance and a potentiostat by recording double-layer capacitance. Contact angle measurements were made with a goniometer (Rame-Hart-300) affixed with a nitrogen-purged environmental chamber. Contact angles were measured for 2-μL drops of both purified water and the cyt *c* adsorption buffer, potassium phosphate solution (4.4 mM, pH = 7), with no statistically significant difference between the two solvents in terms of measured contact angles.

Film thickness estimations were performed as in previous reports[71,72] using the relationship $A = 1000\epsilon_{350}\Gamma$ where the film's absorbance at 350 nm (A) is used with an estimated molar absorptivity (ϵ_{350})[71−73] to calculate a surface coverage (Γ) in nanomole per square centimeter. Surface coverage, in turn, can be converted to an approximate number of monolayers after making assumptions regarding the density and film structure. In this case, a hexagonal close packed model for a layered MPC film ($Au_{225}(C6)_{75}$) was assumed, and calculations were performed for films with both maximum core edge-to-edge spacing ($\Gamma_{MONO} = 2.2 \times 10^{-11}$ mol/cm^2) as well as the expected ∼60% interdigitation ($\Gamma_{MONO} = 3.1 \times 10^{-11}$ mol/cm^2).[74] These calculations, when adjusted for growth on both sides of the glass slide, and the measured Γ can be used to determine the number of MPC monolayers within the film and an estimated thickness. In some cases (i.e., dithiol-linked films), ellipsometry was used to verify the thickness estimations and, as discussed in the text, was found to have excellent agreement. Ellipsometry measurements were performed with a PhE-101 discrete wavelength ellipsometer (Micro Photonics, Inc.) at 632.8 nm.

Synthesis of Hydrophilic MPCs. MPCs with slightly smaller cores but featuring a hydrophilic periphery were created using a modified procedure by Rubinstein et al.[75] In brief, the synthesis involves dissolving 600 mg of tetraoctylammonium bromide (TOABr) in ∼40 mL of toluene. Hydrogen tetrachloroaurate (200 mg) previously dissolved in 20 mL of water was then added, and the mixture was stirred for 5 min. The dark, ruby red organic layer was separated and placed in an ice bath (0 °C) for 30 min while being stirred. Sodium borohydride (200 mg) was dissolved in nanopure water (15 mL) and also chilled to 0 °C before being added quickly to the stirring organic layer. Stirring at 0 °C was continued for 1 to 1.5 h before the organic phase (dark violet) was again separated. This toluene layer, containing TOABr-protected nanoparticles, was then washed with 0.1 M HCL (15 mL), 0.1 M NaOH (15 mL), nanopure water (3×, 15 mL each), and brine solution (20 mL) in consecutive order. A DMF solution (10 mL) of either 6-mercaptohexanol (100 μL) or MUA (250 mg) was briskly stirred while TOABr-capped nanoparticles (20 mL) were added dropwise under N_2. This mixture, which remains violet during the addition of TOABr-capped nanoparticles, was stirred for an additional 2 h before being evaporated to near dryness (∼1 mL) under vacuum. 2-Propanol (10 mL) was added to the slurry, and it was reconcentrated to ∼1 mL. The remaining solid was precipitated out four successive times by adding 2-propanol (0.5 mL) and acetone (30 mL), and the product was collected by centrifugation each time. The final product, verified with UV−vis spectroscopy, NMR, and TEM analysis (Supporting Information), was dried on a vacuum line overnight and used within a week.

Cytochrome *c* Purification. Cyt *c* (Sigma) was purified using established protocols.[22] Briefly, an as-received solution of cyt *c* was prepared (5 mg in 2 mL of 4.4 mM KPB) and passed through a cation-exchange column (CM-32, Whatman) with 70 mM KPB as an elution solvent. Fractions of the second reddish band were collected, combined, and concentrated using an Amicon filtration system (YM-10 membrane). The concentrated sample of cyt *c* in 70 mM KPB was eluted from a P6-DG desalting column (BioRad) and concentrated with the same Amicon filtration system. Protein solutions, typically 5−12 μM in 4.4 mM KPB as determined from its UV−vis spectrum, were used within 1 to 2 weeks after purification and checked periodically for denaturation.

Electrochemistry. Cyclic voltammetry, including capacitance measurements, was performed with CH Instruments potentiostats (model 650A or 610B) with both a low current amplifier and a Faraday cage. The aforementioned evaporated gold substrates served as the working electrodes in a previously described inverted cell design (Supporting Information) that also features a platinum counter electrode, a Ag/AgCl (saturated KCl) reference electrode (Microelectrodes, Inc.). An electroactive surface area of the gold electrode of 0.32 cm^2 was defined by a Viton O-ring.

Double layer capacitance (C_{dl}) determinations were executed by considering the film as a whole since solvent is mostly excluded from the inner architecture of the film. Double-layer theory indicates that such a film can then be modeled as a parallel plate capacitor with the planes of charge (i.e., the electrode surface and the outer Helmholtz plane at the film/solution interface) separated by a dielectric layer composed of the film itself.[30,65] To calculate double layer capacitance for a film, the total current (I_{Tot}) of a voltammetry scan was measured at 120 mV vs Ag/AgCl and the following equation was applied:

$$C_{dl}(\mu F/cm^2) = \frac{I_{Tot}}{(2 \cdot v \cdot A) \times 10^{-6}}$$

where v is the sweep rate (V/s) and A is the area of the working electrode (cm^2). A value of 120 mV was chosen for C_{dl} determination because of a lack of Faradaic current in that potential range. Apparent ET rate constants ($k_{ET}°$) were determined by applying Laviron's kinetic model for adsorbed species where quasi-reversible voltammetry of cyt *c* was induced by increasing scan rates until peak splitting was ≥200 mV.[76]

Results and Discussion

The following results are focused on the two major factors of PME systems that contribute to high electrochemical signal-to-noise ratios: (1) effective discrimination of background current or capacitance and (2) control of interfacial properties for immobilization of native protein material at the surface.[14] Specifically, the capacitance of the film assemblies and the ability to control interfacial properties to a degree that systematically affects protein adsorption and subsequent electrochemistry are investigated.

Capacitance of MPC Film Assemblies (Non-Faradaic Background). Networked films of MPCs with a variety of linking mechanisms have been previously explored in the

(71) Zamborini, F. P.; Leopold, M. C.; Hicks, J. F.; Kulesza, P. J.; Malik, M. A.; Murray, R. W. *J. Am. Chem. Soc.* **2002**, *124*, 8958−8964.
(72) Leopold, M. C.; Donkers, R. L.; Georganopoulou, D.; Fisher, M.; Zamborini, F. P.; Murray, R. W. *Faraday Discuss.* **2004**, *125*, 63−76.
(73) Hicks, J. F.; Seok-Shon, Y.; Murray, R. W. *Langmuir* **2002**, *18*, 2288−2294.
(74) Zamborini, F. P.; Smart, L. A.; Leopold, M. C.; Murray, R. W. *Anal. Chim. Acta* **2003**, *496*, 3−16.
(75) Wanunu, M.; Popovitz-Biro, R.; Cohen, H.; Vaskevich, A.; Rubinstein, I. *J. Am. Chem. Soc.* **2005**, *127*, 9207−9215.
(76) Laviron, E. *J. Electroanal. Chem.* **1979**, *101*, 19−28.

literature, but double layer theory has not yet been applied to such films. To simplify analysis of the double layer of the MPC film assemblies in this study, each film as a whole was modeled as a parallel plate capacitor,[30,65] where the inner and outer Helmholtz planes are defined as being the electrode surface and the film/solution (electrolyte) interface, respectively. The assumption of identifying the outer Helmholtz plane and defining the entire film as a dielectric layer in this model is reasonable considering the extensive literature reports showing these films are not wetted by water and that minimal ion penetration from the supporting electrolyte into the film is expected.[68,71,72] One of the more well-reported MPC film assemblies is that of carboxylic acid-functionalized MPCs linked with carboxylate−metal ion−carboxylate electrostatic bridges. Following established procedures (detailed in the Supporting Information), we were able to assemble films of MUA-modified MPCs with zinc ions serving as metal ion linkers. Films of this nature were grown on both silanized glass slides and MUA SAM-modified gold electrodes with the multilayer assembly tracked via UV−vis spectroscopy and cyclic voltammetry, respectively. The spectra of the films during assembly (Figure 2A) show that there is a steady increase in absorbance with each growth cycle (i.e., exposure to both linker and MPC solutions). Cyclic voltammetry of the film at each stage of assembly (Figure 2B) shows a corresponding increase in charging current as the film is grown thicker. This result is not surprising considering it is well-established that MPCs behave as tiny capacitors featuring an electron-rich, polar core surrounded by an insulating periphery[77,78] and that a single growth cycle (dip) of metal-linked films results in multilayers of deposited MPCs.[66,67] In spite of their protective hydrocarbon layers, the mere presence of the cores also introduces a polarizable entity into the double layer of the film, subsequently raising the dielectric constant of the material. Thus, on the basis of the combination of these two factors in this model, a steady increase in C_{dl} as these films are assembled is expected.

As previously mentioned, a key component of achieving well-defined protein monolayer electrochemistry is the effective discrimination against the background signal or charging current.[14] When cyt *c* was adsorbed to these zinc−carboxylate-linked films, the resulting voltammetry was very poor (Figure 3), and the protein electrochemistry was barely discernible above the background charging current. Aside from the MPC cores themselves, a major contributor to the large capacitance observed with these films is likely due to the increased dielectric of the adlayers that results from the inclusion of metal linkers and carboxylic acid groups, both those involved in linking bridges and those left uncoordinated, throughout the film.[79] With such large, uncompensated background signals, the voltammetry of the adsorbed cyt *c* is ill-defined, though a lack of protein coverage may also be a contributing factor. Regardless, electrochemical properties and surface coverage are not readily attainable with this type of result.

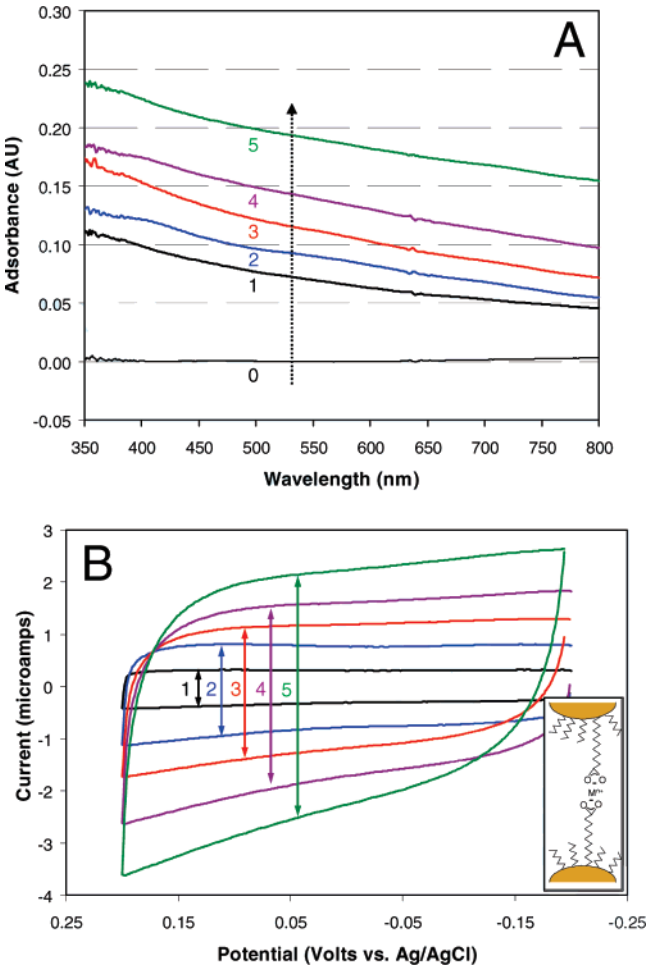

Figure 2. (A) UV−vis spectra tracking the growth of a MPC film assembly on a glass substrate during the first five dipping cycles (numbered) where a cycle consists of immersing the substrate in a solution of MUA-modified MPCs followed by exposure to a solution of linking molecules to establish a linking bridge, in this case a carboxylate−metal ion (Zn^{2+})−carboxylate linkage between neighboring nanoparticles (see inset in B). (B) Cyclic voltammetry of the same type of MPC film assembled on a gold substrate showing the corresponding increase in charging current (background signal) with each dipping cycle (numbered). Voltammetry was recorded at 100 mV/s in 4.4 mM potassium phosphate buffer (pH = 7).

In an attempt to understand the C_{dl} of MPC films, the cyclic voltammetry of films employing alternative linking mechanisms was explored. MPC films assembled with ester coupling and dithiol covalent linkages have been presented in the literature, and details of our assembly procedures are provided in Supporting Information. These linking mechanisms are attractive here in that they do not rely on the incorporation of metal ions into the MPC film architecture. For our initial attempt at forming these metal-free films, separate solutions of acid or alcohol functionalized MPCs were made via exchange reactions between the hexanethiol-protected MPCs and either MUA or 11-mercaptoundecanol (MUD) ligands, respectively. Following established procedures, an ester-coupled MPC film is grown by alternating and sequential exposures (i.e., dips) of the substrate to solutions of MUD MPC and MUA MPC in the presence of ester-coupling reagent and catalyst. Unlike the growth of the metal-linked films which deposits multiple layers with each dip,[66,67] the ester-coupled film is believed to be more

(77) Chen, S.; Murray, R. W.; Feldberg, S. W. *J. Phys. Chem. B* **1998**, *102*, 9898−9907.
(78) Pietron, J. J.; Hicks, J. F.; Murray, R. W. *J. Am. Chem. Soc.* **1999**, *121*, 5565−5570.
(79) Films of this nature have freely diffusing and uncoordinated metal ion linkers throughout their structure.[66,67] If metal cations are able to migrate to the interface, it is likely that they would disrupt the electrostatic immobilization of the protein, thereby causing lower protein coverage and serving as a significant factor in the poorly defined protein voltammetry (Figure 3).

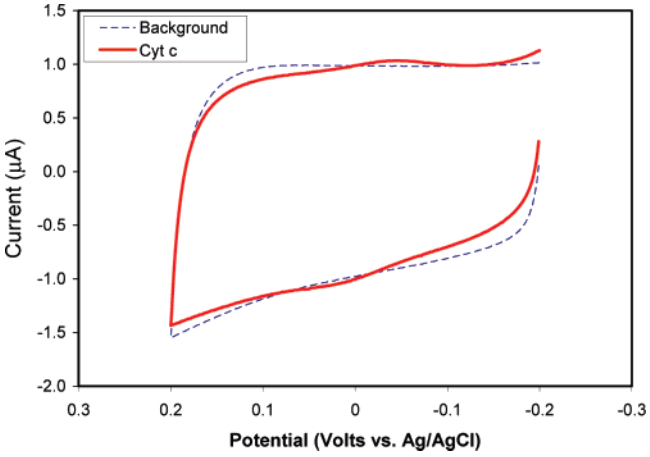

Figure 3. Cyclic voltammetry of a Zn^{2+}-linked MUA MPC film with (solid line) and without (dashed line) adsorbed cyt *c*. The signal of the cyt *c* is obscured by the poorly compensated background signal. Voltammetry was recorded at 100 mV/s in 4.4 mM potassium phosphate buffer (pH = 7).

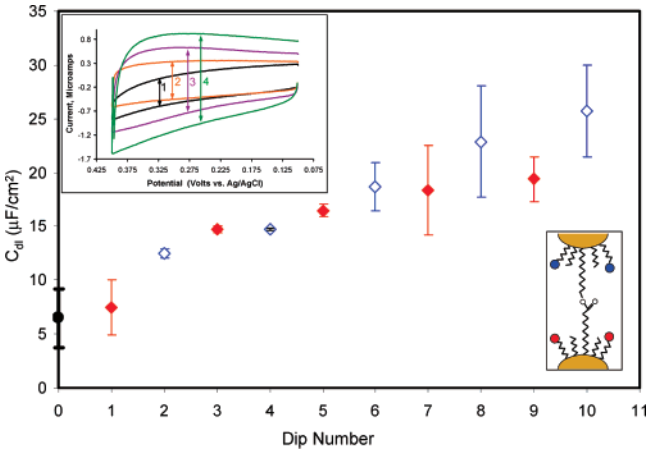

Figure 4. C_{dl} of ester-coupled MPC film assemblies monitored over 10 dip cycles that include alternating exposure of the modified substrate to hydroxy-functionalized MPCs (red ◆) or carboxylic acid-functionalized MPCs (◇) in the presence of ester-coupling reagents. The initial C_{dl} (●) is shown for the initial MUA/MHDA mixed SAM used to anchor the film. Inset: Representative cyclic voltammetry of ester-coupled MPC films through the first four dipping cycles. Voltammetry was recorded at 100 mV/s in 4.4 mM potassium phosphate buffer (pH = 7).

consistent with layer-by-layer growth.[68,80] The capacitance of the film was monitored with cyclic voltammetry and tracked over each of the dipping cycles (Figure 4). These results clearly indicate that each exposure to the functionalized MPCs brings about a corresponding increase in capacitance, evident from the increase of charging current observed in each successive voltammogram. Moreover, starting from the measurement of the initial anchoring SAM on the substrate, the capacitance appears to steadily increase with each dip cycle in a specific pattern. As alternating layers of acid or alcohol functionalized MPCs are ester-coupled into the film, the capacitance appears to increase more abruptly with the addition of MUA MPCs to the film compared to the MUD MPCs. In this case, the high polarity of the carboxylic acids, coupled with the sensitivity of the material's dielectric constant to the presence of polarizable groups, may explain this observation. Nevertheless, the C_{dl} of the ester-coupled MPC films, like that of the metal-linked films,

(80) Hicks, J. F.; Young, S.; Murray, R. W. *Langmuir* **2002**, *18*, 2288−2294.

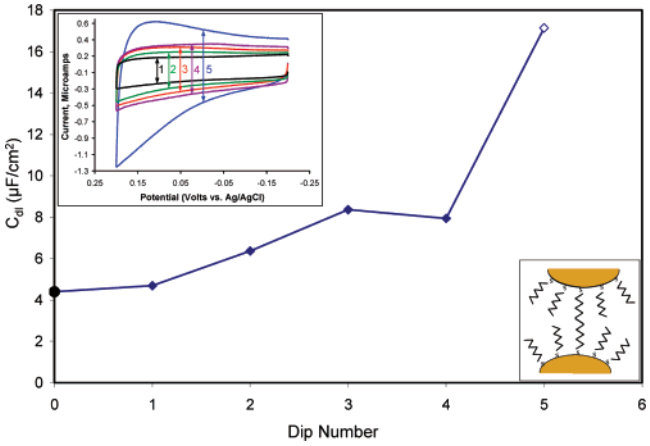

Figure 5. C_{dl} of dithiol-linked MPC film assemblies on a modified gold substrate monitored over five dipping cycles. After the fourth exposure to a solution of unfunctionalized MPC (blue ◆), the substrate was exposed to a final, fifth dip of carboxylic acid-functionalized MPC (◇), resulting in a sharp spike in the observed C_{dl}. The initial C_{dl} (●) is shown for the hexanethiol/nonanedithiol mixed SAM used to anchor the film. Inset: Corresponding cyclic voltammetry of the dithiol-linked MPC film on a gold substrate illustrating the subtle increases in C_{dl} with dithiol-linked layers of MPC as well as the substantial increase observed with exposure to a functionalized MPC.

appears to contribute a significant background signal, most likely because of the excess hydroxyl and carboxylic acid groups within the film that are not involved with ester coupling.

To test if the capacitance of the film was sensitive to the presence of polarizable groups, we targeted dithiol linkages between hexanethiol-protected MPCs. With a completely covalent linking bridge that is also hydrophobic like the MPC's periphery, films with dithiol linkages would seem to present a material with an inherently lower dielectric constant. Again, MPCs were assembled on a mixed SAM (i.e., hexanethiol with nonanedithiol) modified gold substrate using dithiols to construct the film layer-by-layer while the C_{dl} was measured. Figure 5 summarizes the voltammetry and capacitance data for the growth of the dithiol-linked film. In this case, the increase in C_{dl} with each exposure to MPC was clearly less than the other films as a result of eliminating polar groups within the film. The remaining increase in C_{dl} per dip is largely attributed to capacitive properties of the MPCs within the film. To help confirm the role of polarizable groups in the capacitance of the film, MUA-modified MPC was added as a final layer to the dithiol-linked film. As expected, the capacitance suddenly increases with the addition of this layer, an increase uncharacteristic of the previous growth trend with unfunctionalized MPCs (Figure 5).

Figure 6 provides a summary comparison of the MPC films assembled with metal−carboxylate, ester-coupled, and dithiol-linking mechanisms. The equations for linear regression are included to illustrate the significant difference in the C_{dl} of these films per dip number (slope). While all three types of films exhibit an increase in C_{dl} during assembly, it is clear from the trends that the linking mechanism has a profound influence on the overall property of the film, including the charging current, a property directly related to the background signal in PME. If these films are to be used as platforms for PME, the dithiol-linked films represent the most promising architecture by exhibiting only a modest increase in capacitance with the assembly of several layers of MPC.

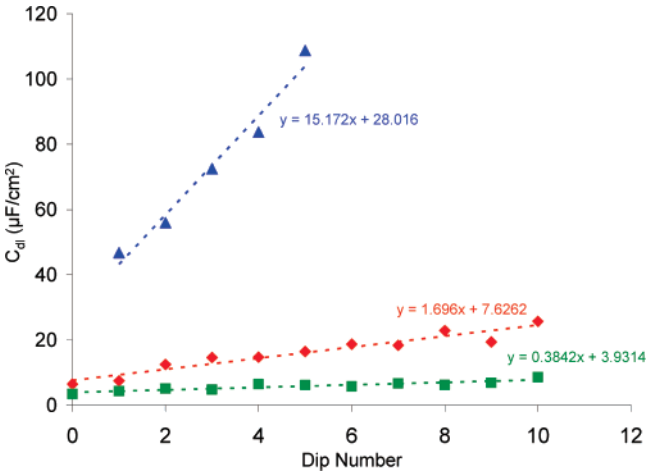

Figure 6. Comparison of the C_{dl} for metal-linked (blue ▲), ester-coupled (red ◆), and dithiol-linked (green ■) MPC films during assembly.

All the results discussed above were obtained with films composed of hexanethiolate (C6)-protected MPCs with an *average* composition of $Au_{225}(C6)_{75}$ as a base material. Once the linking mechanism yielding the lowest C_{dl} was identified, experiments designed to find the optimal core size and protecting ligand in terms of C_{dl} were carried out. To determine the optimal core size, dithiol-linked films of hexanethiolate-protected nanoparticles with core sizes of Au_{140}, Au_{225}, and Au_{807} were grown and measured for capacitance.[81] Likewise, the optimal chain length of protecting ligands was determined by holding the core constant at Au_{225} and constructing films of those particles with protective ligands of varying chain lengths (from 4-mercaptobutane to 10-mercaptodecane) while monitoring C_{dl} during film growth. The results of these experiments are shown and discussed in Supporting Information. On the basis of the results of these optimization experiments, films composed of $Au_{225}(C6)_{75}$ showed a more optimal combination of handling/growth properties, solubility, and lower capacitance compared to nanoparticles composed of other core sizes or protecting ligand chain lengths. It should be noted, however, that these factors, chain length and core size, were much less substantial contributors to overall film capacitance than the linking mechanism employed within the film. Thus, the primary focus of our discussion regarding the background signal centered on how linking mechanism affects film capacitance. The remainder of our study, exploring the protein interface of the films, utilizes dithiol-linked films of $Au_{225}(C6)_{75}$ exclusively.

Interfacial Protein Adsorption and Electrochemistry (Faradaic Signal). As illustrated in Scheme 1, the standard film assembly for PME includes the deposition of four layers of MPCs to mask the gold topography followed by a final layer specifically designed to immobilize cyt *c*. AFM of the gold substrates before and after the five layers of MPC are assembled (Supporting Information) confirms that there is no major change to the micrometer-scale topography of the substrates. Of interest in these systems is the surface concentration (Γ), electrochemical properties, and stability (i.e., resistance to denaturation) of the immobilized protein. One major goal of our effort was to see if rational design of the nanoparticle before being incorporated into the film translates into interfacial control of protein adsorption and activity once the specifically engineered MPCs became the film's final layer. To illustrate this concept, we first produced MPC samples with varying amounts of MUA ligands to act as the final binding layer of the films. MPCs with an average composition of $Au_{225}C6_{75-N}(MUA)_N$, where N varied in a range from 21 to 58, were synthesized and attached as the fifth layer to MPC films. The average number of MUA (N) on the MPCs, verified by NMR analysis of iodine-decomposed samples, was created by systematically varying parameters of the exchange reactions, including time of reaction and the amount of MUA ligand added to the mixture. MPC film assemblies featuring the fifth layer with varying number of MUA were exposed to solutions of cyt *c* and tested for the voltammetric response of the adsorbed protein. The results of these experiments, shown in Figure 7, indicate that significant control of the interface of these films is achieved by manipulating the properties of the MPCs in the final layer of the films. As the number of average MUA per MPC is increased, the voltammetric peaks of the cyt *c* signal become more defined and the surface concentration (Γ) of adsorbed protein, measured by integrating the anodic or cathodic wave, increases. It follows that higher MUA content allows for a greater number of binding sites as well as an increase in the hydrophilic nature of the interface (vide infra for more information).

The cyt *c* voltammetry at the varying MUA MPC films was repeatedly measured to monitor changes in surface coverage over several days. The traditional system of cyt *c* adsorbed to a carboxylic acid-terminated SAM, in this case MUA SAM, is known to be stable for several days with little decrease in peak amplitude due to denaturation of the protein. Cyt *c* adsorbed to our MPC films, however, showed both a lower initial surface coverage and a relatively accelerated rate of denaturation compared to the traditional system over a time span of 5 days (Figure 8). The results indicate that the coverage of protein as well as its denaturation rate is dependent on the number of MUA groups at the adsorption interface. We suspect that the hydrophobic character of the interface, resulting from the hexanethiolate protecting ligands remaining on the MPCs, is likely accelerating denaturation of the protein at the surface. This idea is reinforced by contact angle measurements of these films compared to both hydrophobic and hydrophilic SAMs (Supporting Information). The contact angles, while more hydrophilic with increasing number of MUA groups, are still largely hydrophobic and not conducive for sustaining native protein at the surface.

To further reinforce this observation, MPCs to be incorporated as the film's interfacial layer were designed with varying chain lengths of the protecting ligands. MPCs were first synthesized with a range of protecting ligand chain lengths, including butanethiol (C4), hexanethiol (C6), octanethiol (C8), decanethiol (C10), and dodecanethiol (C12). Each of these individual MPCs were then exchanged with MUA ligands under the same conditions used to generate the samples in the previous figure with approximately 58−60 MUA ligands per MPC, a material we hereafter designate as "Max-MUA-MPC". After the exchange reactions, these samples were collected and used as fifth

(81) The range of sizes of MPC cores is chosen so that their size is similar to the diameter of the protein targeted for immobilization on their surface. In this case, cyt *c* is 35 Å in diameter,[29] whereas the diameters of the MPCs examined in the study, including their alkanethiolate perpipheral ligands, are estimated to be 5.4, 5.8, and 6.6 nm for $Au_{140}C6_{53}$, $Au_{225}C6_{75}$, and $Au_{807}C6_{163}$, respectively. MPC diameters are predicted by theoretical modeling of the most probable cores sizes[60] and are consistent with the TEM analysis of our materials (Supporting Information).

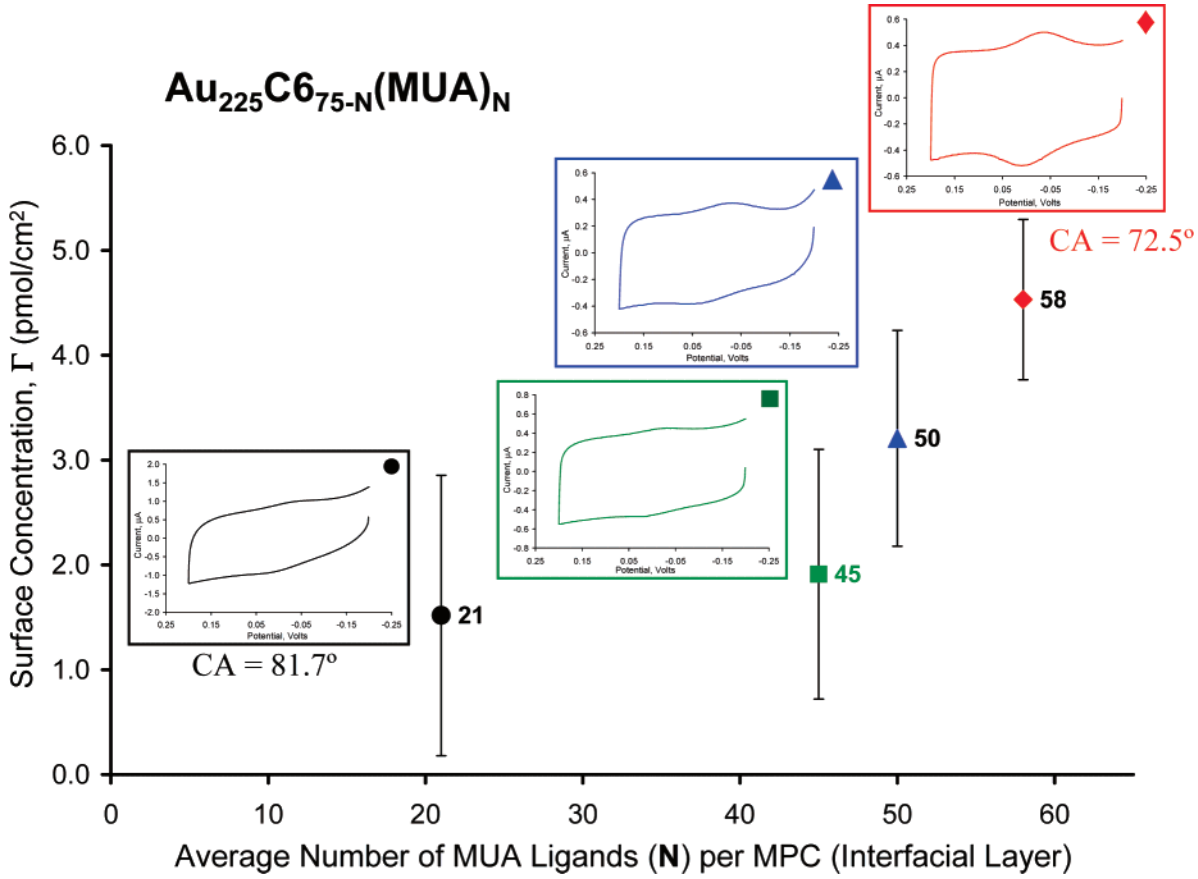

Figure 7. Surface concentration (Γ) of cyt *c* at dithiol-linked MPC film assemblies with a final layer composed of MPCs with an average composition of $Au_{225}C6_{75-N}(MUA)_N$, where *N* represents the average number of MUA ligands per MPC in the interfacial layer. Insets: Corresponding cyclic voltammetry of cyt *c* at films featuring a final layer of MPCs with varying number of MUA ligands. Voltammetry was recorded at 100 mV/s in 4.4 mM potassium phosphate buffer (pH = 7). Contact angles (CA) are shown for films featuring MPCs with an average of 21 and 58 MUAs to illustrate the changing hydrophobic nature of the interface.

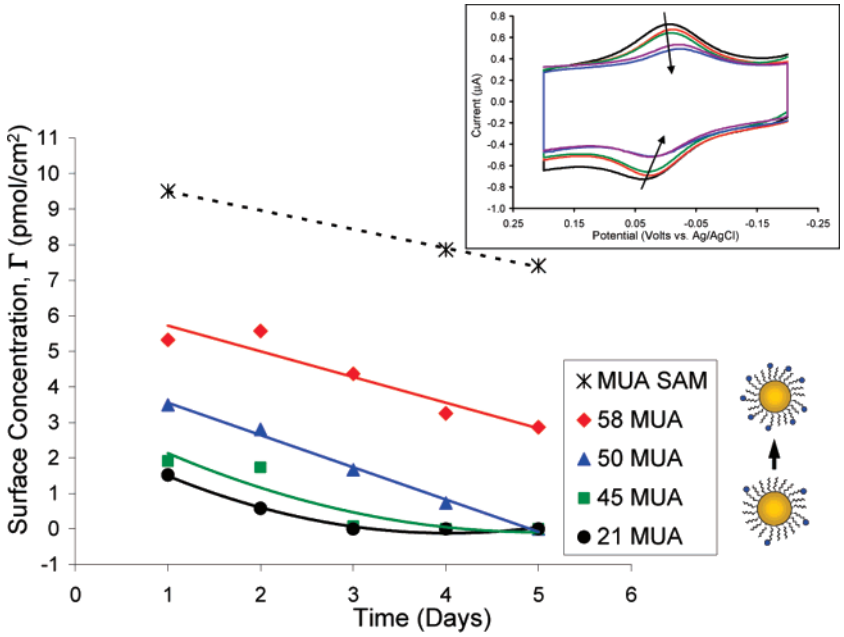

Figure 8. Surface concentration (Γ) of cyt *c* at dithiol-linked MPC film assemblies with varying MUA ligands in the final layer tracked over 5 days. Inset: Corresponding cyclic voltammetry of cyt *c* at a 58 MUA MPC film assembly showing denaturation of the protein (decreasing coverage) over time. Voltammetry was recorded at 100 mV/s in 4.4 mM potassium phosphate buffer (pH = 7).

layers of MPC films and then exposed to a solution of cyt *c*. Figure 9 shows the results of the cyt *c* voltammetry on these systems in terms of both peak shape/definition (A) as well as quantitative values of Γ over time (B). As the chain length of the nonbinding ligands rivals that of MUA, adsorption is either eliminated (C12) or severely diminished with accelerated

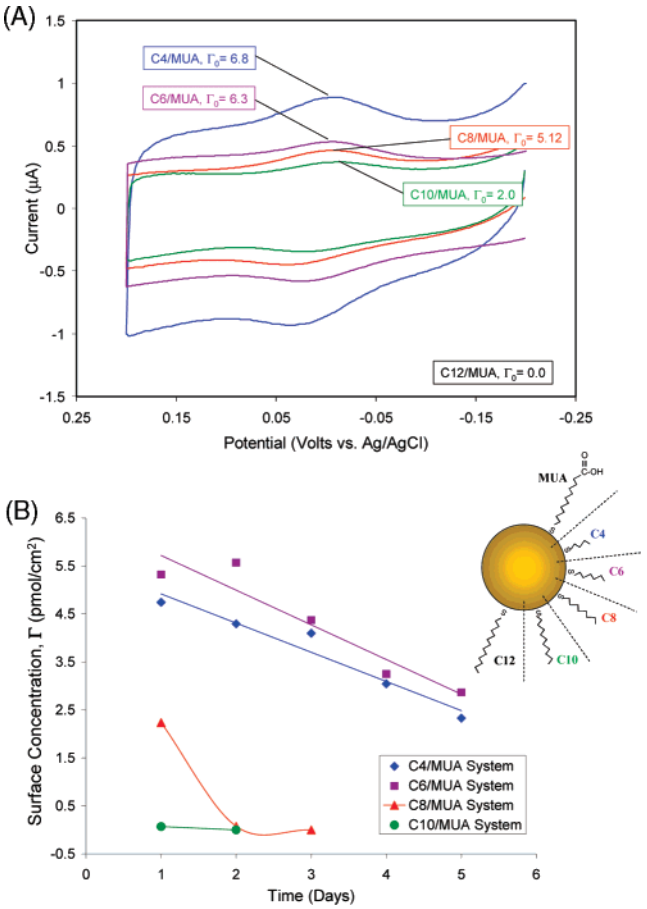

Figure 9. (A) Typical cyclic voltammograms of cyt *c* at MPC film assemblies with interfacial layers of MPCs affixed with MUA ligands and varying chain lengths of nonlinking alkanethiolates, including butanethiolate (C4), hexanethiolate (C6), octanethiolate (C8), decanethiolate (C10), and dodecanethiolate (C12). Note: The average composition of the MPCs in these experiments was designed as $Au_{225}CX_{75-N}(MUA)_N$, where N is approximately 45.[63,82] Voltammetry was recorded at 100 mV/s in 4.4 mM potassium phosphate buffer (pH = 7). (B) Average surface concentration (Γ) of cyt *c* at these varying chain lengths MPC film tracked over 5 days. Inset: Illustration of the MPCs designed for the chain length experiments to test for adsorption and denaturation.

Scheme 2. Hydrophilic MPCs Used as Fifth Layers of Film Assemblies

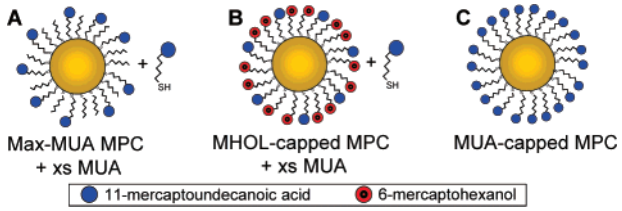

denaturation, most easily observed with the C8 and C10 systems. C4 and C6 systems show higher initial coverage, more defined voltammetry, and greater resistance to denaturation.[82] It is noteworthy to point out that the inverse relationship between hydrocarbon chain length and C_{dl} is observable from the voltammetry in Figure 9A. As the chain length of the unfunctionalized alkanethiolate component in the MPC periphery is increased (C4 → C10), the C_{dl} of the film expectedly decreases because the film assembly as a whole possesses a higher content of hydrocarbons with a lower dielectric constant.

While significant control over the interface was achieved in the above experiments, the denaturation rate and low surface coverage were not satisfactory for determining if the nanoparticles were inducing more ideal cyt *c* adsorption (i.e., decreased dispersion of electrochemical properties). Considering the experimental evidence present that suggests that these factors, coverage and denaturation, may be directly related to the lack of hydrophilic carboxylic acid binding sites at the interface, we specifically engineered materials to compensate for this possibility. After four layers of dithiol-linked, unfunctionalized MPCs were assembled, several strategies were employed to create more hydrophilic nanoparticles to serve as the final layer of the films. In the first method, normal place-exchange reactions resulting in Max-MUA-MPCs were carried out as described. The product of this reaction, however, was not precipitated and washed as before. The exchange reaction solution, comprising both the Max-MUA-MPCs and excess (xs), uncoordinated MUA ligands, was instead used as the final dip solution (Scheme 2A). It is believed that the fifth layer of MPC with high percentages of surface MUA would be immobilized while the free MUA ligands would be further exchanged into the film, resulting in a much more hydrophilic interface. Indeed, the contact angle of a water droplet at a film prepared in this manner was 45°, markedly lower (more hydrophilic) than the previous films made without free MUA present during fifth layer deposition (Supporting Information).

The second and third type of strategy used to create a more hydrophilic interface involved synthesizing purely hydrophilic MPCs. Using adaptations to a procedure developed by Rubinstein et al. (Experimental Details),[75] we were able to generate both 6-mercaptohexanol (MHOL) and MUA-capped MPCs. The MHOL MPCs were applied as a fifth layer as described in the preceding paragraph where a four-layer film was treated with a solution mixture of MUA-exchanged MHOL MPCs and xs MUA ligands to generate a more hydrophilic fifth layer (Scheme 2B). Likewise, completely MUA-capped MPCs were also synthesized and used as prepared (i.e., without excess MUA) as a fifth layer (Scheme 2C).

MPC film assemblies were constructed with each of these three types of hydrophilic layers and exposed to cyt *c* solutions. The resulting electrochemistry immediately after the cyt *c* adsorption (i.e., day 1) and changes in surface coverage over 5 days are shown in Figure 10. Figure 10 compares the results from these three hydrophilic interfaces (green ▲, purple ■, blue ●) with the most optimal, Max-MUA-MPC system of Figure 8 (red ◆, bottom), and with a traditional system of cyt *c* adsorbed to a MUA SAM (*, top). Initially, the highly exchanged Max-MUA-MPCs with xs MUA resulted in a high surface coverage, equal to the coverage found at the MUA SAM. After the first day, however, a relatively sharp denaturation rate was observed before normalizing after 3 days. The reasons for this abrupt, yet repeatable, decrease remain undefined.[83] The voltammetry of the system on that first day (Figure 10, inset, green ▲) does

(82) Exchange reaction parameters (reaction time and MUA concentration) were carefully manipulated to create MPCs with similar *average* MUA content as verified by the NMR analysis of iodine decomposed samples. However, chain-length effects on the propensity of MUA in solution to exchange/displace surface thiolates cannot be completely dismissed since the C12/MUA system consistently showed low MUA content regardless of the exchange reaction parameters.

(83) One possible explanation for this occurrence may be that, with the MUA ligands significantly longer than the hexanethiolates in a mixed peripheral layer, there may be some bending of the chains that exposes the hydrophobic methylene units and subsequently accelerates denaturation of the protein.

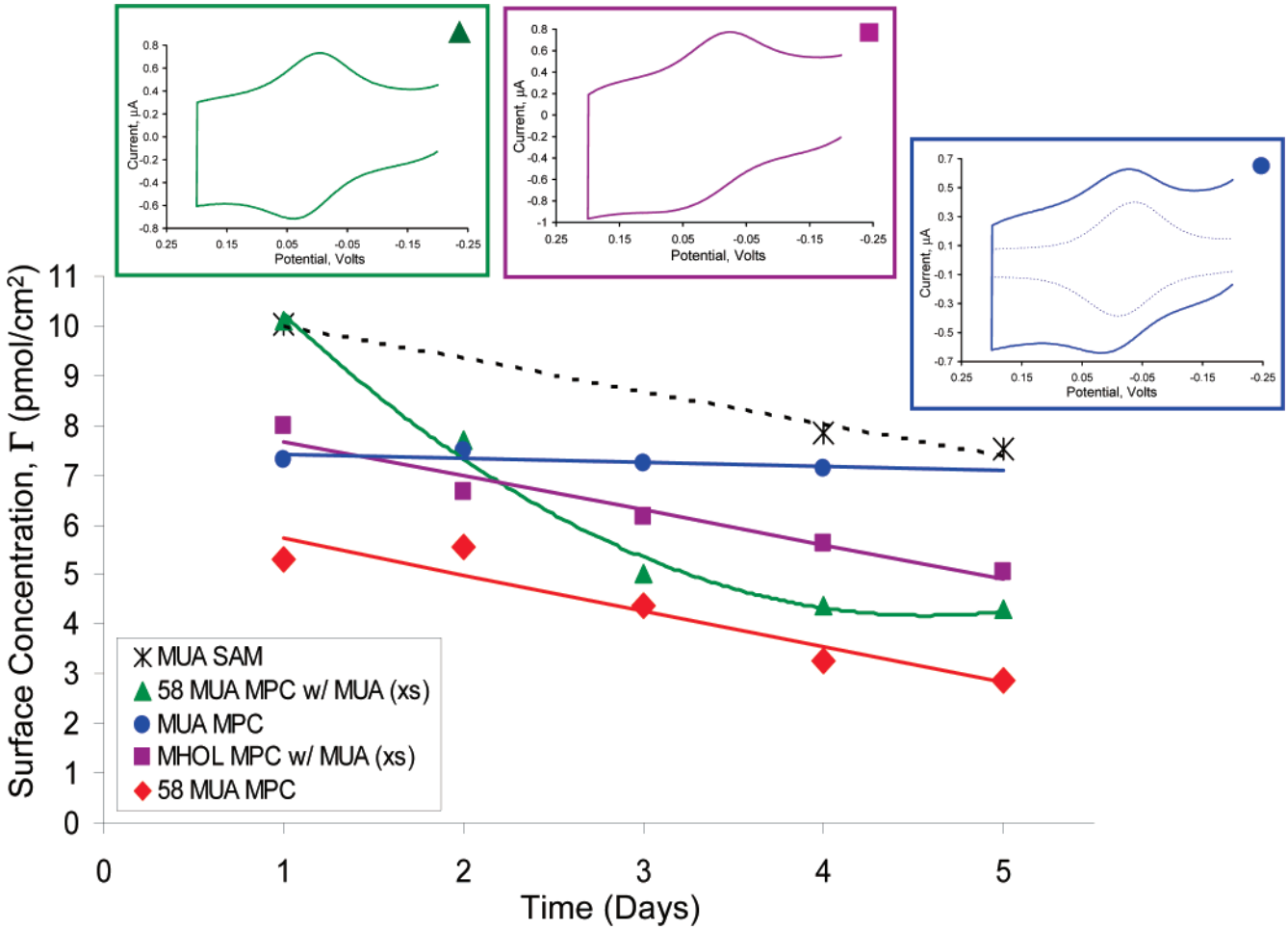

Figure 10. Surface concentration (Γ) of cyt *c* at dithiol-linked MPC film assemblies with a final layer composed of various types of MPCs including those with an average composition of $Au_{225}C6_{17}(MUA)_{58}$ (red ◆), $Au_{225}C6_{17}(MUA)_{58}$ attached as a fifth layer in the presence of excess MUA ligands (green ▲), MHOL-capped MPCs attached as a fifth layer in the presence of excess MUA ligands (purple ■), and MUA-capped MPCs (blue ●). All of these systems are also compared to a traditional system of cyt *c* adsorbed to a MUA SAM (*). Insets: Corresponding cyclic voltammetry of cyt *c* at films featuring a final layer of hydrophilic MPCs (green ▲, purple ■, blue ●). The voltammetry of cyt *c* at a traditional MUA SAM systems is included in the last inset for comparison. Voltammetry was recorded at 100 mV/s in 4.4 mM potassium phosphate buffer (pH = 7).

reveal cyt *c* oxidation and reduction waves that are easily discernible from the background and represents the first example of well-defined protein monolayer electrochemistry at an MPC film assembly of this nature and rivals the peak definition of the traditional SAM system.

The purely hydrophilic systems of MHOL MPCs with xs MUA and the MUA MPCs both resulted in higher coverage than the systems with the most MUA ligands per MPC (red ◆) but is slightly lower than that for the Max-MUA-MPC with xs MUA. For the MHOL MPC films, the denaturation rate is similar to that of the prior hydrophilic system tested above. More importantly, similar to other hydrophilic interfaces, the MHOL MPCs with xs MUA result in well-defined voltammetry (Figure 10, inset, purple ■). The pure MUA MPC system yields high coverage with the slightest denaturation rate of any system tested over a 5-day period. The voltammetry of this system (Figure 10, inset, blue ●), shown in comparison with a traditional MUA SAM system, is extremely well-defined peaks above the background signal, making it the most successful system to date.

With higher coverage and well-defined voltammetry at the MPC films, we turned our attention to the original goal of using nanoparticles to control interfacial properties to a degree where more ideal PME was achieved. Table 1 lists the electrochemical properties of two traditional SAM systems compared to those of several of the MPC film assemblies investigated in this study. The electrochemical properties of the cyt *c* at the SAMs are in excellent agreement with literature reports for typical monolayer coverages of cyt *c* and illustrate the anomalous peak broadening, most easily detected by larger fwhm values, inherent in these systems.[20,31] In this study, the fwhm values for the MUA and 16-mercaptohexadecanoic acid (MHDA) SAM systems are clearly expanded beyond the ideal value of 90 mV,[30] yielding 127 and 146 mV, respectively. As previously mentioned, the broadening of these peaks has been attributed to heterogeneous adsorption of protein, with individual cyt *c* molecules experiencing different adsorption environments that result from a lack of molecular level control at the interface. When the electrochemical parameters of the three hydrophilic MPC systems are compared to those of the traditional systems, a significant decrease in the fwhm occurs, and some of the MPC assemblies (green ▲) even yield close to ideal fwhm values of 90, 91, and 93 mV. The difference in fwhm of the MUA SAM system compared to all three hydrophilic-capped MPC film assemblies is statistically significant at 95% confidence,[84] suggesting that the nanoparticles are successfully controlling the interfacial chemistry and providing a more uniform adsorption platform

Table 1. Electrochemical Properties of Cyt *c* at Various Hydrophilic MPC Assemblies/SAMs[a]

system/fifth layer	$E^{\circ\prime}$ volts	ΔE_p volts	Γ pmol/cm^2	fwhm volts	k_{ET}° s^{-1}
MUA SAM	−0.027	0.024	11.1	0.127	6.4
	(±0.031)	(±0.011)	(±1.8)	(±0.007)	(±3.3)
MHDA SAM	−0.035	0.181	8.9	0.146	0.3
	(±0.010)	(±0.028)	(±0.3)	(±0.008)	(±0.2)
MPC MUA (58) w/xs MUA	−0.013	0.067	10.1	0.107	2.7
	(±0.008)	(±0.015)	(±2.7)	(±0.006)	(±0.9)
MHOL MPC w/xs MUA	−0.020	0.066	8.6	0.119	3.1
	(±0.003)	(±0.012)	(±2.3)	(±0.004)	(±1.2)
MUA MPC	−0.027	0.039	7.6	0.112	6.8
	(±0.004)	(±0.012)	(±2.1)	(±0.006)	(±3.6)

[a] Note: xs MUA indicates that the hydrophilic MPCs were synthesized and then mixed with excess MUA ligands to create a mixture that was then inserted into the cells as a fifth layer.

for cyt *c*. We believe the average fwhm values of these hydrophilic MPC systems would approach ideality to a greater degree and be even more reproducible if the polydispersity of the MPC samples was more carefully controlled. This hypothesis has been tested with a crudely fractionated sample of MPCs (verified with TEM analysis) that were subsequently place-exchanged to create a more monodisperse sample of $Au_{225}C6_{17}$-$(MUA)_{58}$. When used as a fifth layer, this material yielded fwhm values for cyt *c* peaks that were on average 100 (±5) mV, nominally 10 mV lower compared to the same experiment performed with unfractionated material.

One of the more interesting features using MPC film assemblies in PME is illustrated by the kinetic parameters that were recorded for these systems, including average peak splitting (ΔE_p) and ET rate constants (k_{ET}°) as determined by application of Laviron's theory[76] (Experimental Details). As shown in Table 1, the ΔE_p of the two SAM systems, MUA and MHDA, shows that the oxidation/reduction of cyt *c* at the longer chain SAM is, as expected, more challenged, with average ΔE_p of approximately 24 mV versus 180 mV, respectively. Moreover, the MUA and MHDA systems differ by an order of magnitude in k_{ET}° with the rate dropping 20-fold on the longer chain film. The values of k_{ET}° for cyt *c* at each of the hydrophilic-capped MPC film assemblies, however, are strikingly similar to those of cyt *c* at the MUA SAM even though the ET distance is significantly greater (i.e., 8−9 times larger). The values of k_{ET}° observed for cyt *c* at films terminated with either Max-MUA-MPC (xs MUA) or MHOL MPC (xs MUA) were both only about 2-fold slower than the same protein at the MUA SAM and an order of magnitude faster than the rate at an MHDA SAM. Moreover, there was no statistically significant difference (95% confidence, two-tailed *t* test)[84] in the rate constants of cyt *c* at the MUA-capped MPC film assemblies (6.8 ± 3.6 s^{-1}) compared to the same protein at MUA SAMs (6.4 ± 3.3 s^{-1}). The significance of these results lies in the extreme difference in ET distance between the SAMs and MPC film assemblies (vide infra for more detail regarding ET distances).

MUA SAMs, assuming a 30° tilt angle and close-packed structure, have been studied with ellipsometry and reported in the literature as being approximately 1.5-nm thick.[65] As described in the Experimental Details, theoretical estimates of the thickness of the MPC film assemblies were calculated on the basis of the average increase in absorbance per dipping cycle measured during dithiol-linked MPC film growth. On the basis of these estimations, the average increase in thickness with each dip was determined to be ∼2.5 nm/dip if the film is interdigitated and ∼4.2 nm/dip if the film is not interdigitated (i.e., MPCs are connected at the length of the nonanedithiol linker). For the film assemblies utilized in this study to immobilize cyt *c* (five dipping cycles), film thicknesses would be estimated at 12.6 nm (interdigitated) and 20.7 nm (not interdigitated). Independent ellipsometry measurements of dithiol-linked MPC film assemblies indicated that the films grew at an average of 2.7 (±0.2) nm/dip, making the films in this study approximately 13.5 (±0.9) nm thick. This measurement supports the idea that the dithiol-linked MPC films not only have an interdigitated structure, but also grow in an approximate layer-by-layer fashion as opposed to the multilayer growth known to occur with other linking mechanisms. Thus, the ET is occurring at similar rates although the protein is an order of magnitude further away from the electrode surface. This impressive result is interpreted in terms of the accelerated "electron hopping" known to occur in MPC film assemblies featuring electron self-exchange rate constant between MPCs on the order of 10^6 s^{-1}.[85−87] This result has implications not only for fundamental PME systems but also for long-range ET applications such as increasing the signal of amperiometric biosensor designs incorporating nanoparticles with advanced architectures.

Conclusions

We have reported the successful incorporation of MPCs as a functional component of PME systems and a viable strategy for creating a uniform, large area platform that can also be easily optimized for specific protein adsorption through manipulations of interfacial properties and flexibility on a molecular level. By carefully investigating and optimizing the electrochemistry of cyt *c* at MPC film assemblies, it was shown that well-defined and more ideal voltammetry compared to the SAM systems could be achieved through specifically engineering the properties of the MPCs and the MPC film. These results are attributed to three major factors that were addressed within this body of work. First, the background signal or charging current is effectively controlled and discriminated against by manipulating the

(84) Statistical hypothesis testing of the difference in mean samples was performed as a one tail, standardized Student's *t* test, assuming nonhomogeneous variance and a conservative estimate of the degrees of freedom.

(85) Hicks, J. F.; Zamborini, F. P.; Osisek, A. J.; Murray, R. W. *J. Am. Chem. Soc.* **2001**, *123*, 7048−7053.
(86) Hicks, J. F.; Zamborini, F. P.; Murray, R. W. *J. Phys. Chem. B* **2002**, *106*, 7751−7757.
(87) Brennan, J. L.; Branham, M. R.; Hicks, J. F.; Osisek, A. J.; Donkers, R. L.; Georganopoulou, D. G.; Murray, R. W. *Anal. Chem.* **2004**, *76*, 5611−5619.

properties of the MPCs (core size, chain length) and the linking mechanism used within the film. The result of this manipulation allows for greater voltammetric peak resolution and defined background compared to other reports[47−51,88] where protein is adsorbed to electrodes modified with water-soluble materials such as citrate-stabilized nanoparticles. Second, the topography of the gold substrate, a known contributor to interfacial heterogeneity and subsequent nonideal adsorption,[32] is effectively negated with the buildup of a thicker modifying layer on the electrode as confirmed by ellipsometry. Even though there is a drastic increase in distance between the adsorbed protein and the electrode surface, the ET is mediated by the presence of the nanoparticles, resulting in rate constants normally observed at much thinner SAM adlayers. The impressive kinetics of PME at MPC films may be used in the future to exceed monolayer coverage since the modified layers can be made larger (e.g., branched over a larger distance) without losing the electrochemical signal. The third and probably most influential attribute of these MPC films is that they allow for a greater degree of molecular level control over the intricate and diverse nanoenvironment required for optimal protein adsorption.[89−91] Through various procedures, MPCs can be easily manipulated to exhibit specific interfacial properties, including a range of hydophobicity, flexibility, and functionality at the protein binding site that are both more uniform and more optimized for adsorption. AFM imaging shows no morphological change to the substrate's microscopic topography, suggesting topographical control on the nanoscale, more relevant to the protein's size. On the basis of our results, we propose that more ideal electrochemical behavior is achieved with proteins adsorbed to MPC films because there is a greater probability that the proteins will experience, *on a molecular level*, a more homogeneous adsorption environment compared to more traditional, modified substrates.

In the future, we will explore how MPC film assemblies of this nature can be further optimized, allowing for an even greater control over interfacial properties conducive to more consistent high protein coverage, low rates of denaturation, and near-ideal adsorbed voltammetric behavior. Obtaining MPC samples with lower polydispersity will be a primary focus of this effort since it should provide for an even more uniform protein adsorption platform. Likewise, more intricate manipulations of the MPC's peripheral ligand structure and functionality will be examined, including branched ligands or those with hydrophilic functional groups incorporated in their chains. Both types of ligands may reduce the lateral hydrophobic interactions we suspect are affecting the adsorbates in these current films. For now, we present MPC film assemblies as an effective strategy for controlling interfacial properties of protein adsorption platforms that can be easily applied to a large surface area without regard to the substrate topography and resulting in more ideal electrochemical behavior. It is our hope that this work elucidates how the unique and easily manipulated properties of nanoparticles can be applied to a variety of bioanalytical applications.

Acknowledgment. We gratefully acknowledge the American Chemical Society Petroleum Research Fund (42161-GB5) and the Thomas F. Jeffress and Kate Miller Jeffress Memorial Trust for generously supporting this research. Additional support is appreciated from the Howard Hughes Medical Institute (A.F.L. and K.P.R.) and the Camille and Henry Dreyfus Foundation (A.F.L.). We thank Christopher Kidd and Christie Bredahl for their work on this project and Dr. Carolyn Marks (University of Richmond, Biology Department) for her technical support with TEM, Dr. Matt Trawick (University of Richmond, Physics Department) for his help with AFM analysis of the substrates, and Dr. Kevin Kittredge (Sienna College) with Rong Zhang (Miami University, OH) for ellipsometry analysis of our materials.

Supporting Information Available: Procedural details for assembling the different MPC film assemblies and AFM analysis of the substrates, TEM analysis of different MPC core sizes, C_{dl} growth trend for metal-linked MPC film assembly, core size/chain length C_{dl} optimization results, and characterization (UV−vis, NMR, TEM) of MUA-capped MPCs. This material is available free of charge via the Internet at http://pubs.acs.org.

JA076312K

(88) Yi, X.; Huang-Xian, J.; Hong-Yuan, C. *Anal. Biochem.* **2000**, *278*, 22−28.
(89) Roach, P.; Farrar, D.; Perry, C. C. *J. Am. Chem. Soc.* **2006**, *128*, 3939−3945.
(90) Yue, H.; Khoshtariya, D.; Waldeck, D. H.; Grochol, J.; Hildebrandt, P.; Murgida, D. H. *J. Phys. Chem. B* **2006**, *110*, 19906−19913.
(91) Asuri, P.; Karajanagi, S. S.; Yang, H.; Yim, T.; Kane, R. S.; Dordick, J. S. *Langmuir* **2006**, *22*, 5833−5836.